# Dynamic Regulation of miRNA Expression by Functionally Enhanced Placental Mesenchymal Stem Cells Promotes Hepatic Regeneration in a Rat Model with Bile Duct Ligation

Jae Yeon Kim[1], Ji Hye Jun[1], Soo Young Park[1], Seong Wook Yang[2], Si Hyun Bae[3] and Gi Jin Kim[1,*]

[1] Department of Biomedical Science, CHA University, Seongnam, 13488, Republic of Korea; janejaeyeon92@gmail.com (J.Y.K.); jihyejun1015@gmail.com (J.H.J.); soobookpark@gmail.com (S.Y.P.); gjkim@cha.ac.kr (G.J.K.)

[2] Department of Systems Biology, College of Life Science and Biotechnology, Yonsei University, Seoul, 120749, Republic of Korea; yangsw@yonsei.ac.kr (S.W.Y.);

[3] Department of Internal Medicine, Catholic University Medical College, Seoul, 03312, Republic of Korea; baesh@catholic.ac.kr (S.H.B.)

[*] Correspondence: gjkim@cha.ac.kr; Tel.: +82-31-881-7145

**Abstract:** Placenta-derived mesenchymal stem cells (PD-MSCs) have been highlighted as therapeutic sources in several degenerative diseases. Recently, microRNAs (miRNAs) were mediated one of the therapeutic mechanisms of PD-MSCs in regenerative medicine. To enhance the therapeutic effects of PD-MSCs, we established functionally enhanced PD-MSCs with phosphatase of regenerating liver-1 overexpression (PRL-1(+)). However, the profile and functions of miRNAs induced by PRL-1(+) PD-MSCs in a rat model with hepatic failure prepared by bile duct ligation (BDL) remained unclear. Hence, the objectives of the present study were to analyze the expression of miRNAs and investigate their therapeutic mechanisms for hepatic regeneration via PRL-1(+) in a rat model with BDL. We selected candidate miRNAs based on microarray analysis. Under hypoxic conditions, compared with invaded naïve PD-MSCs, invaded PRL-1(+) PD-MSCs showed improved integrin-dependent migration ability through RHO family-targeted miRNA expression (e.g., hsa-miR-30a-5p, 340-5p, and 146a-3p). Moreover, rno-miR-30a-5p and 340-5p regulated engraftment into injured rat liver by transplanted PRL-1(+) PD-MSCs through the integrin family. Additionally, an increase in PDGFRA by suppressing rno-miR-27a-3p improved vascular structure in rat liver tissues after PRL-1(+) PD-MSCs transplantation. Furthermore, decreased rno-miR-122-5p was significantly correlated with increased proliferation of hepatocytes in liver tissues by PRL-1(+) PD-MSCs by activating IL-6 signaling pathway through the repression of rno-miR-21-5p. Taken together, these findings improve the understanding of therapeutic mechanisms based on miRNA-mediated stem cell therapy in liver diseases.

**Keywords:** Liver failure; microRNAs (miRNAs); Placenta-derived mesenchymal stem cells (PD-MSCs); Phosphatase of regenerating liver-1 (PRL-1); Regenerative medicine, Stem cells homing; Vascular remodeling

## 1. Introduction

Although the liver has an exceptional regenerative ability, hepatic diseases are induced by several environmental factors, such as viral infection and chemical exposure [1]. Accumulated fibrosis, progressive hepatic vascular pressure, and inflammatory reaction due to continuous hepatic damage are the main causes of liver cirrhosis [2]. In particular, failure of the hepatocyte-endothelium crosstalk in the damaged liver results in abnormal healing, which is shown by the formation of fibrosis or scar tissues [3]. Additionally, the abnormal hepatic vasculature system not only represses metabolic ability but also exhibits fibrotic pathophysiology [4,5]. Presently, orthotopic transplantation of the liver is credited as the only therapeutic surgical method to treat irreversible hepatic failure. However, this operation has many limitations (e.g., insufficiency of donors and the problem of immunity) [6].

Recently, the facilitation of hepatic regeneration in chronic liver injuries by mesenchymal stem cells (MSCs) was shown to be a useful cell therapy source [7,8]. In previous reports, we demonstrated that placenta-derived MSCs (PD-MSCs) have a therapeutic effect on carbon tetrachloride ($CCl_4$)-injured rat liver through antifibrotic, antiapoptotic, and autophagic mechanisms and epigenetic alterations of interleukin-6 (IL-6)/signal transducer and activator of transcription 3 (STAT3) signaling [9,10]. Also, the migration activity of MSCs into injured tissues is an important factor in maximizing their therapeutic effects because transplanted MSCs adhere to the endothelium of vessel and migrate into damaged tissues through chemoattraction [11,12]. We previously demonstrated that PD-MSCs migrated and invaded endothelial cells in a hypoxic environment through Integrin alpha 4 (ITGA4) and RHO signaling [13]. Integrin-dependent signaling activates adhesion to enhance MSC migration into injured target tissues. Additionally, migrated MSCs promote microvessel regeneration in damaged tissues [14]. It is well known that MSCs have angiogenic paracrine effects via secreted molecules, including several growth factors and secretomes, and vascular remodeling, which increase the proliferation and viability of endothelial cells. However, there are still unclear the mode of action of naive MSCs as well as low efficacies of MSCs in degenerative diseases. Due to the reason, many scientists have been tried to develop next-generation stem cells, which have functionally enhanced potentials.

Recently, it was reported that phosphatase of regenerating liver-1 (PRL-1; protein tyrosine phosphatase type IVA, member 1; PTP4A1; PTPCAAX1), which was identified as an immediate early gene, is involved in vascular regeneration by increasing portal flow in a partial hepatectomy model during hepatic regeneration [15] and in mitogenic upregulation [16]. Moreover, PRL-1 induces migration and adhesion by activating c-Src levels [17], and p115 Rho GTPase-activating protein (GAP) binds PRL-1 through the Src homology 3 domain [18]. In particular, miR-26a, miR-944, and miR-601 suppressed cell migration and invasion by targeting PRL-1 [19-21].

MicroRNAs (miRNAs) are small, noncoding, single-stranded RNA sequences, 18-22 nucleotides in length, that regulate diverse cellular processes by binding to the 3'-untranslated region (3'-UTR) of target mRNAs, resulting in mRNA degradation and translational repression [22]. miRNAs are important regulators of stem cells in the treatment of various diseases, such as liver fibrosis [23]. Downregulation of miR-30e expression in a $CCl_4$-induced hepatic fibrosis model by human bone marrow-derived MSCs (hBM-MSCs) resulted in migration ability [24]. Moreover, umbilical cord MSCs (UC-MSCs) transplantation reduced the severity of hepatic fibrosis in a $CCl_4$-injured mouse model through the suppression of miR-199 expression targeted to the 3'-UTR site of keratinocyte growth factor mRNA to decrease translation [25].

However, the profile and functions of the miRNAs that mediate liver regeneration following the administration of functionally enhanced PD-MSCs with PRL-1 overexpression (PRL-1(+)) to the bile duct ligation (BDL)-injured rat model remain unclear. Therefore, the major objective of the study was to analyze the expression patterns of miRNAs and to investigate miRNA-mediated therapeutic effects on hepatic regeneration on the engraftment of PRL-1(+) PD-MSCs through changes in adhesion molecules and angiogenic factor-targeted miRNAs in a rat model with BDL.

## 2. Results

### *2.1. miRNA Profiling of Invaded Naïve PD-MSCs Under Hypoxic Conditions and in BDL-Injured Liver in Rats*

To determine miRNA-mediated regulation of the migration ability of PD-MSCs, we assessed the microarray of invaded naïve PD-MSCs under hypoxic conditions and from the liver samples of

rats with BDL administered naïve PD-MSCs at 1 and 2 weeks. First, the mRNA expression profile revealed significantly increased hypoxia-inducible factor 1 alpha (HIF1A) and vascular endothelial growth factor (VEGF) in the invaded naïve PD-MSCs under hypoxic conditions compared with those under normoxic conditions (Figure 1A, $^{*}p<0.05$). In the microarray data, 57 miRNAs were detected in invaded naïve PD-MSCs under hypoxic conditions and in BDL-injured rat liver samples transplanted with MSCs. We found the 2 miRNAs were downregulated and 18 miRNAs were upregulated under hypoxic conditions compared with normoxic conditions (Hyp/Nor), in the transplanted naïve (TTx Naïve) group at 1 week compared with the nontransplanted (NTx) group at 1 week (TTx/NTx 1w), and in the TTx Naïve group at 2 weeks compared to the NTx group at 2 weeks (TTx/NTx 2w). Moreover, we identified 3 downregulated miRNAs and 34 upregulated miRNAs shared by the Hyp/Nor and TTx/NTx 1w comparisons and 9 downregulated miRNAs and 25 upregulated miRNAs shared by the Hyp/Nor and TTx/NTx 2w comparisons. Also, we identified 3 downregulated miRNAs and 26 upregulated miRNAs shared by the TTx/NTx 1w and TTx/NTx 2w comparisons (Figure 1B, C). The data suggested that the miRNA profiles of naïve PD-MSCs with migration ability under hypoxic conditions and of BDL-injured rat liver samples were identical.

### *2.2. PRL-1-Dependent Migration Ability Under Hypoxic Conditions Regulated by miRNAs Targeting the Integrin Family*

To investigate whether invaded PD-MSCs with PRL-1(+) regulate adhesion-related molecules for cell migration, we assessed mRNA and targeting miRNA expression in invaded PD-MSCs with PRL-1(+) under hypoxic conditions. We analyzed the migration ability of naïve PD-MSCs and PD-MSCs with PRL-1(+) using a transwell insert system. Increased HIF1A and VEGF levels were confirmed in invaded PD-MSCs with PRL-1(+) under hypoxic conditions compared with those under normoxic conditions (Figure 2A, $^{*}p<0.05$). Interestingly, the mRNA expression of PRL-1 was increased in invaded naïve PD-MSCs under hypoxia compared with those under normoxia. Moreover, hypoxia-treated PRL-1(+) PD-MSCs are higher PRL-1 expression than normoxia. We found that the hsa-miR-30a-5p binding site is conserved in the 3'-UTR of the PRL-1 mRNA. hsa-miR-30a-5p expression clearly matched the mRNA expression of PRL-1 in naïve and PRL-1(+) PD-

MSCs under hypoxic conditions (Figure 2B, $^{\#}p<0.05$). The invaded naïve PD-MSCs showed decreased ITGA4 expression under hypoxic conditions compared with normoxic conditions. The evidence supported our previous report that decreased ITGA4 expression controls the migration ability of hypoxic naïve PD-MSCs [13]. On the other hand, PRL-1(+) PD-MSCs exposed to hypoxia had a significant increase in ITGA4 expression. The targeting of hsa-miR-340-5p to ITGA4 was confirmed (Figure 2C, $^{\#}p<0.05$). Additionally, integrin beta 7 (ITGB7) expression in naïve PD-MSCs was higher under hypoxia than under normoxia. Interestingly, we found that PRL-1(+) PD-MSCs under hypoxia had remarkably increased ITGB7 mRNA levels. Moreover, hsa-miR-146a-3p expression was capable of more markedly downregulating the expression of ITGB7 in PRL-1(+) PD-MSCs than in naïve (Figure 2D, $^{\#}p<0.05$). These results suggest that the hypoxia-mediated migration ability of PRL-1(+) PD-MSCs regulates miRNAs through the integrin family.

### *2.3. PRL-1-Targeted miRNA Expression Regulates Migration Ability Through the RHO Family*

Interestingly, we found that PRL-1(+) PD-MSCs had increased migration ability under hypoxic conditions compared with normoxic conditions. Therefore, we hypothesized that PRL-1 may be positively related to migration ability. To confirm the function of PRL-1 in the migration of PD-MSCs, we used siRNA-PRL-1 (siPRL-1) treatment to knock down PRL-1 expression. The number of invaded PRL-1(+) PD-MSCs was higher than that of naïve. On the other hand, in the invasion of naïve and PRL-1(+) PD-MSCs was significantly decreased with siPRL-1 treatment (Figure 3A, B, $^{\#}p<0.05$). Moreover, we verified PRL-1 expression with or without siPRL-1 treatment. hsa-miR-30a-5p expression was decreased in invaded PRL-1(+) PD-MSCs compared to invaded naïve PD-MSCs. The knockdown of PRL-1 induced increased hsa-miR-30a-5p levels (Figure 3C, $^{\#}p<0.05$). The expression levels of ras homolog family member A (RHOA) and rho-associated coiled-coil-containing protein kinase 1 (ROCK1) were significantly increased in invaded PRL-1(+) PD-MSCs and without siPRL-1 treatment compared to invaded naïve PD-MSCs. Following siPRL-1 treatment, the mRNA expression levels of RHOA and ROCK1 were clearly attenuated in naïve and PRL-1(+) PD-MSCs (Figure 3D, $^{\#}p<0.05$). The data demonstrate that PRL-1-dependent miR-30a-5p regulates migration through the RHO family.

155

156 *2.4. Integrin Family Regulates miRNA Expression for PRL-1(+) PD-MSC Homing in vivo in a Rat*
157 *Model with BDL*

158 One function of MSCs is efficient stem cell homing and migration into injured target tissue
159 for therapy [26]. Activated integrin family, RHOA and downstream factor ROCK regulate MSC
160 adhesion and migration by regulating phosphorylated focal adhesion kinase (FAK) [27]. Therefore,
161 we confirmed that the integrin family regulates miRNA expression for stem cell engraftment in a
162 BDL-injured rat model. After each MSC transplantation, the human-specific Alu sequence in cirrhotic
163 liver samples from each rat group was confirmed using quantitative real-time polymerase chain
164 reaction (qRT-PCR) analysis. Compared to the Non-transplantation (NTx) group, the tail-vein
165 transplantation (TTx) Naïve group had increased human-specific Alu expression. Interestingly, we
166 found that compared to the TTx Naïve group, the TTx PRL-1(+) group exhibited a remarkable
167 increase in Alu level (Figure 4A, $^{\#}p<0.05$). Consistently, ITGA4 and ITGB7 expression in the TTx
168 PRL-1(+) group was significantly increased compared to the TTx Naïve group (Figure 4B, $^{\#}p<0.05$).
169 We searched for differences in hsa-miR-30a-5p and rno-miR-30a-5p. Although hsa-miR-30a-5p
170 targets PRL-1 mRNA, rno-miR-30a-5p targets integrin alpha 6 (ITGA6) in miRNA-target prediction
171 databases (http://www.mirdb.org and http://www.targetscan.org). rno-miR-340-5p also targets
172 integrin beta 1 (ITGB1). The mRNA level of ITGA6 was decreased in the NTx group compared to the
173 TTx group. rno-miR-30a-5p was increased in the NTx groups compared with the TTx groups except
174 at 1 week. Interestingly, ITGA6 expression was significantly increased in the TTx PRL-1(+) group
175 compared with the TTx Naïve group by repressing rno-miR-30a-5p level (Figure 4C, $^{\#}p<0.05$).
176 Moreover, the ITGB1 expression of the TTx PRL-1(+) group was remarkably improved compared to
177 that of the NTx and TTx Naïve groups by suppressing rno-miR-340-5p level (Figure 4D, $^{\#}p<0.05$).
178 The results suggested that the integrin family regulates miRNA expression for engraftment into
179 injured liver by PRL-1(+) PD-MSC transplantation in a rat model with BDL.

180

*2.5. Improved Vascular Remodeling by PRL-1(+) PD-MSCs Through the Regulation of miRNA Expression by PDGFRA in a BDL-injured Rat Model*

Generally, vascular structure and their functions in tissues are one of important factors to maintain homeostasis of organs. However, they are changed to abnormal conditions when they exposed to stress or damaged conditions. So, abnormal vascular structures in damaged liver tissues are common evidences. To analyze vascular remodeling following the transplantation of naïve and PRL-1(+) PD-MSCs into a BDL rat model, we confirmed the expression and localization of angiogenic factors. Compared to that in the NTx group, the mRNA expression of endoglin (ENG) in the TTx Naïve group was increased at 2 and 3 weeks. Interestingly, compared with the TTx Naïve groups, the TTx PRL-1(+) group had significantly improved ENG expression and platelet-derived growth factor receptor beta (PDGFRB) level (Figure 5A, B, $^{\#}p<0.05$). Furthermore, the PDGF receptor alpha (PDGFRA)-targeted rno-miR-27a-3p was significantly repressed in the TTx Naïve group at 2, 3, and 5 weeks and the TTx PRL-1(+) group at 1, 2, and 3 weeks compared to the NTx group. In contrast to the expression of rno-miR-27a-3p, the expression pattern of PDGFRA in the TTx PRL-1(+) group was remarkably increased (Figure 5C, $^{\#}p<0.05$). To investigate the localization and expression of PDGFRA in BDL rat liver tissues transplanted with PRL-1(+) PD-MSCs, we performed immunofluorescence assays. PDGFRA was localized in the membrane of liver sinusoidal endothelial cells and in the hepatic nucleus. In particular, the expression of PDGFRA was upregulated in the TTx PRL-1(+) group compared with the NTx and TTx Naïve groups (Figure 5D). These results indicate that vascular remodeling is improved by PRL-1(+) PD-MSCs through the PDGFRA-mediated regulation of miRNA expression in a rat model of BDL.

*2.6. miRNAs Mediated Hepatic Regeneration by PRL-1(+) PD-MSCs in a Rat Model with BDL through IL-6/STAT3 Signaling*

To determine whether the administration of PRL-1(+) PD-MSCs could induce liver regeneration by regulating miRNAs, interleukin-6 (IL-6)/signal transducer and activator of transcription 3 (STAT3) signaling, which is a representative pathway that promotes liver regeneration and well-known cytokine of hepatocyte protection, the expression of mRNA, protein, and regulating

miRNAs was confirmed in rat livers with BDL-injured model. We examined whether PRL-1(+) PD-MSCs promoted hepatocyte proliferation in rat BDL-injured livers, and proliferating cell nuclear antigen (PCNA) immunohistochemistry was used to analyze liver tissues. The mRNA expression of interleukin 6 receptor (IL-6R) was increased in the TTx Naïve group compared with that the NTx group at 2 and 5 weeks. Interestingly, compared with the TTx Naïve groups, the TTx PRL-1(+) groups had significantly improved IL-6R levels. rno-miR-21-5p-targeted IL-6R expression was downregulated in the TTx Naïve group at 2, 3, and 5 weeks and in the TTx PRL-1(+) group at 1 and 2 weeks compared with the NTx group (Figure 6A, $^{\#}p<0.05$). We analyzed the protein levels of IL-6 and glycoprotein 130 (gp130), which is a type I cytokine receptor of IL-6, and the phosphorylation level of STAT3 in rat BDL-injured liver. Although the gp130 level showed no significant differences among the groups except for in the sham control (Con) group, the expression of endogenous IL-6 and phosphorylated STAT3 in the liver was higher in the TTx Naïve group than in the NTx group at 1 week. In particular, the TTx PRL-1(+) group had equally improved IL-6 and phosphorylated STAT3 levels compared with the TTx Naïve group (Figure 6B). Furthermore, to analyze the transcription factors involved in the liver regeneration of rats with BDL-injured liver, the mRNA expression levels of HNF1 homeobox A (HNF1A) and hepatocyte nuclear factor 4 alpha (HNF4A) were measured and were found to be increased in the TTx Naïve group compared with the NTx group. Prominent increases in HNF1A and HNF4A expression were observed in the TTx PRL-1(+) group compared to the TTx naïve group. rno-miR-122-5p, which is a representative liver-enriched miRNA that targets HNF1A in the TTx groups, also caused downregulated expression in the TTx groups compared with the NTx group. In particular compared with the TTx Naïve group, the TTx PRL-1(+) group showed remarkably decreased expression of rno-miR-122-5p (Figure 6C, D, $^{\#}p<0.05$). Consistently, to confirm the proliferation of hepatocytes following the transplantation of PRL-1(+) PD-MSCs, we analyzed immunohistochemical staining for PCNA in rat liver tissues. The largest number of PCNA-positive hepatocyte was observed in the TTx PRL-1(+) group, followed by the TTx Naïve and NTx groups (Figure 6E, F, $^{\#}p<0.05$). These data indicate that PRL-1(+) PD-MSCs may regulate miRNA-mediated hepatic regeneration through IL-6/STAT3 signaling.

## 3. Discussion

Mesenchymal stem cells (MSCs) have promising potential in regenerative medicine, including self-renewal, differentiation, and immunomodulatory effects [28,29]. Recent studies revealed that the modulation of miRNA by MSCs is involved in the therapeutic effect between MSCs and injured tissues [30]. In our study, miRNA candidates for stem cell engraftment and vascular remodeling were selected because they were involved in invaded placenta-derived MSCs (PD-MSCs) under hypoxic conditions as well as bile duct ligation (BDL)-injured rat livers at 1 and 2 weeks post-transplantation and had demonstrated effects on liver regeneration (Figure 1). First, integrin-dependent targeting miRNAs (e.g., hsa-miR-30a-5p, has-miR-340-5p, and has-miR-146a-3p) were selected. Target genes were searched in miRNA databases (http:// www.mirdb.org and http://www.targetscan.org).

Generally, the migration of MSCs under low oxygen concentrations is affected by the altered integrin expression and cell-to-cell adhesion [31]. Our previous reports confirmed that invaded naïve PD-MSCs under hypoxia showed decreased integrin alpha 4 (ITGA4) and increased integrin beta 7 (ITGB7) expression for homing effects through the RHO family [13]. In bone marrow-derived MSCs (BM-MSCs), hypoxia inducible factor 1 alpha (HIF1A)-induced microenvironment factors, including hypoxia and ITGA4 expression, impacting the migration ability of BM-MSCs [32]. We confirmed that ITGA4 expression under hypoxia was decreased in naïve PD-MSCs by suppressing hsa-miR-340-5p. Interestingly, compared with naïve, PRL-1(+) PD-MSCs under hypoxia significantly increased both ITGA4 and ITGB7 expression (Figure 2). These data are well matched with the characteristics of PRLs (e.g., PRL-1, PRL-2, and PRL-3), which identically promote cell migration and invasion [33-35]. In general, integrin-mediated adhesion initiated signal transduction by inducing the autophosphorylation of FAK [36,37]. Previous evidence suggested that PRL-1 may regulate the activation of the integrin family. Interestingly, we found that hsa-miR-30a-5p, which targets PRL-1, also regulated ITGA4 and its targeted sequences (Table S3). In addition, we confirmed that the knockdown of PRL-1 decreased migration ability and suppressed hsa-miR-30a-5p though the RHO family (Figure 3). Also, Ma F et al and their colleagues suggested that the targeting of ITGA4 by the hsa-miR-30s family decreased the proliferation of human coronary artery endothelial cells.

Therefore, we hypothesized that PRL-1(+) PD-MSCs in a liver failure model had improved engraftment into targeted injured tissues and mediated repair through MSC migration. To verify this hypothesis, an increase in the human-specific Alu sequence was confirmed after the administration of PRL-1(+) PD-MSCs to a rat model of BDL but not after the administration of naïve PD-MSCs, resulting in ITGA4 and ITGB7 expression. Drescher et al. suggested that the cell migration mediated by the adhesion molecule ITGB7 was involved in the outcome of nonalcoholic steatohepatitis [38]. We confirmed that the targeting of integrin alpha 6 (ITGA6), but not ITGA4, by rno-miR-30a-5p and the targeting of ITGB1, but not ITGA4, by rno-miR-340-5p were significantly repressed in following transplantation with PRL-1(+) PD-MSCs (Figure 4). Human MSC engraftment into the $CCl_4$-injured liver of a murine model regulated ITGB1 in a cluster of differentiation 44 (CD44)-dependent manner [39]. These results are similar with our data.

The transplanted MSCs were found to undergo endothelial transmigration along sinusoidal endothelial cells [40]. A previous study suggested that increased platelet-derived growth factor (PDGF) levels induced liver regeneration by releasing umbilical cord-derived MSCs (UC-MSCs) in a carbon tetrachloride ($CCl_4$)-injured rat model [41]. Moreover, the direct targeting of PDGF receptor beta (PDGFRB) by miR-26b-5p is associated with the negative regulation of angiogenesis and fibrosis in a liver fibrosis model treated with methionine-choline-deficient and high-fat diets [42]. Interestingly, we confirmed that the mRNA expression levels of endoglin (ENG), PDGF receptor alpha (PDGFRA), and PDGFRB induced by PRL-1(+) PD-MSC transplantation in a rat model with BDL were higher than that those induced by transplantation with naïve PD-MSC at 1 week through the suppression of rno-miR-27a-3p and the localization of PDGFRA in the hepatic nucleus and in endothelial cells (Figure 5).

We previously reported the hepatic regeneration induced by naïve PD-MSCs is involved with activated interleukin-6 (IL-6)/signal transducer and activator of transcription 3 (STAT3) signaling and the methylation of inhibited IL-6/STAT3 promoters in a $CCl_4$-injured rat model [10]. We confirmed the protein expression of IL-6/STAT3 in the TTx Naïve and the NTx groups of a rat model with BDL. Interestingly, compared with the TTx Naïve group, the TTx PRL-1(+) group had significantly increased IL-6/STAT3 at 1, 2, and 3 weeks post-transplantation. This result may suggest that PRL-1

led to the phosphorylation of downstream factors, including STAT3, by Src activation for liver regeneration [43]. Additionally, we found that rno-miR-21-5p-targeted interleukin 6 receptor (IL-6R) expression was significantly repressed in the TTx PRL-1(+) group at 1 week and 2 weeks post-transplantation. A previous report indicated that miR-21-5p expression was upregulated in patients with hepatitis B-related acute-on-chronic liver failure compared with controls [44]. These results show a possibility of mo-miR-21-5p as a biomarker for prediction liver regeneration after stem cell therapy. Moreover, miR-122, which is a liver-enriched miRNA, plays a central role in liver function and in the progression of liver disease [45]. In a liver fibrosis model induced by $CCl_4$, miR-122-modified adipose-derived MSCs inhibited collagen accumulation by suppressing the activation of hepatic stellate cells (HSCs) [46,47]. Our result indicated that rno-miR-122-5p-targeted HNF1A, which is a major transcription factor during liver development and regeneration, and PCNA expression in proliferating hepatocytes were dramatically decreased in PRL-1(+) PD-MSCs compared with naïve (Figure 6). However, miRNA expression in rat liver tissues after transplantation with PRL-1(+) PD-MSCs was not the same each week because tissue-specific miRNA patterns vary according to the stage of diseases.

In conclusion, our findings provide clear evidence that PRL-1(+) PD-MSCs promote miRNA-mediated MSC migration under hypoxic conditions through integrin-dependent signaling and promote hepatic regeneration by increased engraftment and vascular remodeling. However, our future studies will consider whether specific miRNAs have strict standards for selection and transfected into PRL-1(+) PD-MSCs recover hepatic function for liver regeneration. These findings will improve the understanding of therapeutic mechanisms based on miRNA-mediated stem cell therapy in liver diseases.

## 4. Materials and Methods

### *4.1. Cell Culture and Gene Transfection*

Placentas from healthy women (≥ 37 gestational weeks) were collected by the Institutional Review Board of CHA Gangnam Medical Center, Seoul, Korea (IRB 07-18). The isolation of naïve PD-MSCs was previously described, their characterization was confirmed, [48,49] and they were

maintained in alpha-modified minimal essential medium (α-MEM; HyClone, Logan, UT, USA) supplemented with 10% fetal bovine serum (FBS; Gibco, Carlsbad, CA, USA), 25 ng/ml human fibroblast growth factor 4 (hFGF4) (PeproTech, Rocky Hill, NJ, USA), 1 μg/ml heparin (Sigma-Aldrich, St. Louis, MO, USA), and 1% penicillin/streptomycin (P/S; Gibco). To overexpress human PRL-1 (phosphatase of regenerating liver-1; protein tyrosine phosphatase type 4 A, member 1; PTP4A1) in naïve PD-MSCs, a PRL-1 plasmid containing the CMV6-AC vector and antibiotic neomycin for mammals was obtained from Origene (Origene Inc., Rockville, MD, USA). Naïve PD-MSCs ($5x10^5$ cells/cuvette) were transfected using the 4D AMAXA Nucleofector™ system (Lonza, Basel, Switzerland). After transfection, the cells were maintained in naïve PD-MSC medium containing 1.5 mg/ml neomycin for selection. Cells were maintained below 5% $CO_2$ at 37 ℃. To induce hypoxia, the cells were placed in a hypoxia chamber and maintained at 1% $O_2$ and 37 ℃.

*4.2. Animal Models and MSC Transplantation*

All animal experimental procedures were approved by the Institutional Animal Care Committee of CHA University, Bundang, Korea (IACUC-190048). Seven-week-old male Sprague-Dawley (SD) rats (Orient Bio Inc., Seongnam, Korea) were used to induce chronic liver cirrhosis by the common BDL model as previously described [50]. The rats were randomly assigned to each of the following groups: sham control (Con; n = 5), BDL-injured nontransplantation (NTx; n = 20), naïve PD-MSC transplantation (TTx Naïve; n = 20), and PRL-1(+) PD-MSC transplantation (TTx PRL-1(+); n = 20). For the administration of each MSC, PKH67-labeled cells were intravenously transplanted into the tail vein. After 1, 2, 3, and 5 weeks, rats from each group were sacrificed, and liver tissues were extracted to analyze therapeutic effects using qRT-PCR, western blotting, and immunostaining.

*4.3. Quantitative Real-time Polymerase Chain Reaction (qRT-PCR)*

Total RNA was isolated from naïve and PRL-1(+) PD-MSCs and rat liver tissues using TRIzol (Invitrogen, Carlsbad, CA, USA). Reverse transcription was performed with 500 ng total RNA and Superscript III reverse transcriptase (Invitrogen). cDNA was amplified by PCR. In the case

of cDNA synthesis for miRNAs, we used the miR-X miRNA First-Strand Synthesis kit (Takara bio, Kusatsu, Shiga, Japan). Real-time PCR was performed using SYBR Master Mix (Roche, Basel, Switzerland) and CFX Connect™ Real-Time System (Bio-Rad, Hercules, CA, USA). Normalization was assessed by human and rat GAPDH for gene expression and U6 for miRNA expression. The sequences of the primers are shown in Tables S1, S2, and S3. All reactions were performed in triplicate.

*4.4. Immunohistochemistry*

To observe the degree of hepatocyte proliferation following transplantation with MSCs or the control, BDL rat liver tissues were stained with anti-PCNA (Santa Cruz Biotechnology, Dallas, Texas, USA) using immunohistochemistry. The liver tissues were embedded in paraffin and sectioned. The sectioned tissues were incubated in 3% $H_2O_2$ in methanol to block endogenous peroxidase activity. After antigen retrieval, the tissues were incubated with a primary antibody (1:200) at 4 ℃ overnight, followed by a 1-h incubation with biotinylated secondary anti-rabbit antibody at room temperature. Incubation with horseradish peroxidase-conjugated streptavidin–biotin complex (DAKO, Santa Clara, CA, USA) and 3,3-diaminobenzidine (EnVision Systems, Santa Clara, CA, USA) was performed to generate a chromatic signal. The samples were counterstained with Mayer's hematoxylin (DAKO). Additionally, the percentage of hepatocytes with PCNA-positive nuclei relative to the total number of hepatocytes was calculated in randomly selected sections using a digital slide scanner (3DHISTECH Ltd., Budapest, Hungary).

*4.5. Immunofluorescence*

To confirm hepatic vascular remodeling following the administration of MSCs or the control, the liver tissues from each group (n = 5) were sectioned into 7-μm thick slices and fixed with 4% paraformaldehyde. The tissue sections were blocked using blocking solution (DAKO) for 1 h under dark conditions. The primary antibody against PDGFRA (1:100; Santa Cruz Biotechnology) was added in a diluent solution (DAKO) at 4 ℃ overnight. The secondary antibody, Alexa Fluor™ 594 goat anti-rabbit IgG (H+L) (1:250; Invitrogen), was reacted for 1 h. The slides from each group were

counterstained with 4',6-diamidino-2-phenylindole (DAPI) (Invitrogen) and observed by confocal microscopy (LSM 700). Images were analyzed with ZEN blue software (ZEISS).

*4.6. Western Blotting*

Homogenized rat liver tissues were lysed in RIPA buffer (Sigma-Aldrich) supplemented with protease inhibitor cocktail (Roche) and phosphatase inhibitor (Sigma-Aldrich). Briefly, 40 μg protein was separated by sodium dodecyl sulfate polyacrylamide gel electrophoresis (SDS-PAGE). The separated proteins were transferred onto PVDF membranes (Bio-Rad). The membranes were incubated with primary antibodies at 4 °C overnight. The following antibodies were used: anti-gp130 (1:500; Santa Cruz Biotechnology); anti-IL-6 (1:1000; Abcam, Cambridge, UK); phospho-STAT3 (1:1000; Cell Signaling Technology, Denvers, MA, USA); and anti-GAPDH (1:3000; Abfrontier, Seoul, Korea). The membranes were then incubated with horseradish peroxidase-conjugated secondary anti-mouse IgG (1:5000, Cell Signaling Technology) and anti-rabbit IgG (1:10000, Cell Signaling Technology) for 1 h at room temperature. Bands were detected using a Clarity Western ECL kit (Bio-Rad).

*4.7. Transwell Migration Assay*

The migration of naïve and PRL-1(+) PD-MSCs was assessed using a Transwell assay. Naïve and PRL-1(+) PD-MSCs ($2x10^4$ cells/well) were seeded onto inserts (8-μm pore size; Corning, NY, USA) with or without siPRL-1 (Integrated DNA Technologies, Coralville, IA, USA) at final concentrations of 50 nM in serum-free medium. The migrated cells in each group were fixed with 100% methanol for 10 min and stained with Mayer's hematoxylin (DAKO). The stained cells in eight random nonoverlapping fields were counted at a magnification of 200X. The experiments were conducted in triplicate.

*4.8. Deep Sequencing and Analysis of Small RNAs*

We performed miRNA sequencing experiments on PD-MSCs using Illumina platforms. We obtained total 10 million clean reads that aligned with the rat genome in the NTx and TTx Naïve at

1 and 2 weeks in rat model with BDL and invaded PD-MSCs under normoxic and hypoxic conditions. We compared the normalized counts of mature miRNAs in NTx versus TTx at 1 week, NTx versus TTx at 2 weeks, and hypoxic versus normoxic conditions. The construction of small RNA libraries with these samples, deep sequencing, and the analysis of small RNAs were performed by LAS Inc. (Gimpo, Republic of Korea). The expression levels of miRNAs (transcripts per 10 million, TPTM) in the indicated samples were calculated by normalizing the miRNA counts with the total number of clean reads in the small RNA libraries.

*4.9. Statistical Analysis*

The data are expressed as the mean ± standard deviation of at least three independent experiments. Student's t-test was conducted, and $p < 0.05$ was considered statistically significant.

**Author Contributions:** J.Y.K (Jae Yeon Kim) and J.H.J (Ji Hye Jun) contributed equally to this work. J.Y.K, J.H.J, and J.Y.K, J.H.J, S.Y.P (Soo Young Park) performed the experiments. S.H.B (Si Hyun Bae) and S.W.Y (Seong Wook Yang) contributed to materials/analysis tools. J.Y.K and J.H.J prepared the manuscript drafting. G.J.K (Gi Jin Kim) conceived and designed the experiments, and directed manuscript drafting, financial support and final approval of manuscript designed the experiments. All authors read, revised, and approved the final manuscript.

**Funding:** This research was supported by a grant of the Korea Health Technology R&D Project through the Korea Health Industry Development Institute (KHIDI), funded by the Ministry of Health & Welfare, Republic of Korea (grant number : HI16C1559, HI17C1050).

**Conflicts of Interest:** The authors declare no conflict of interest.

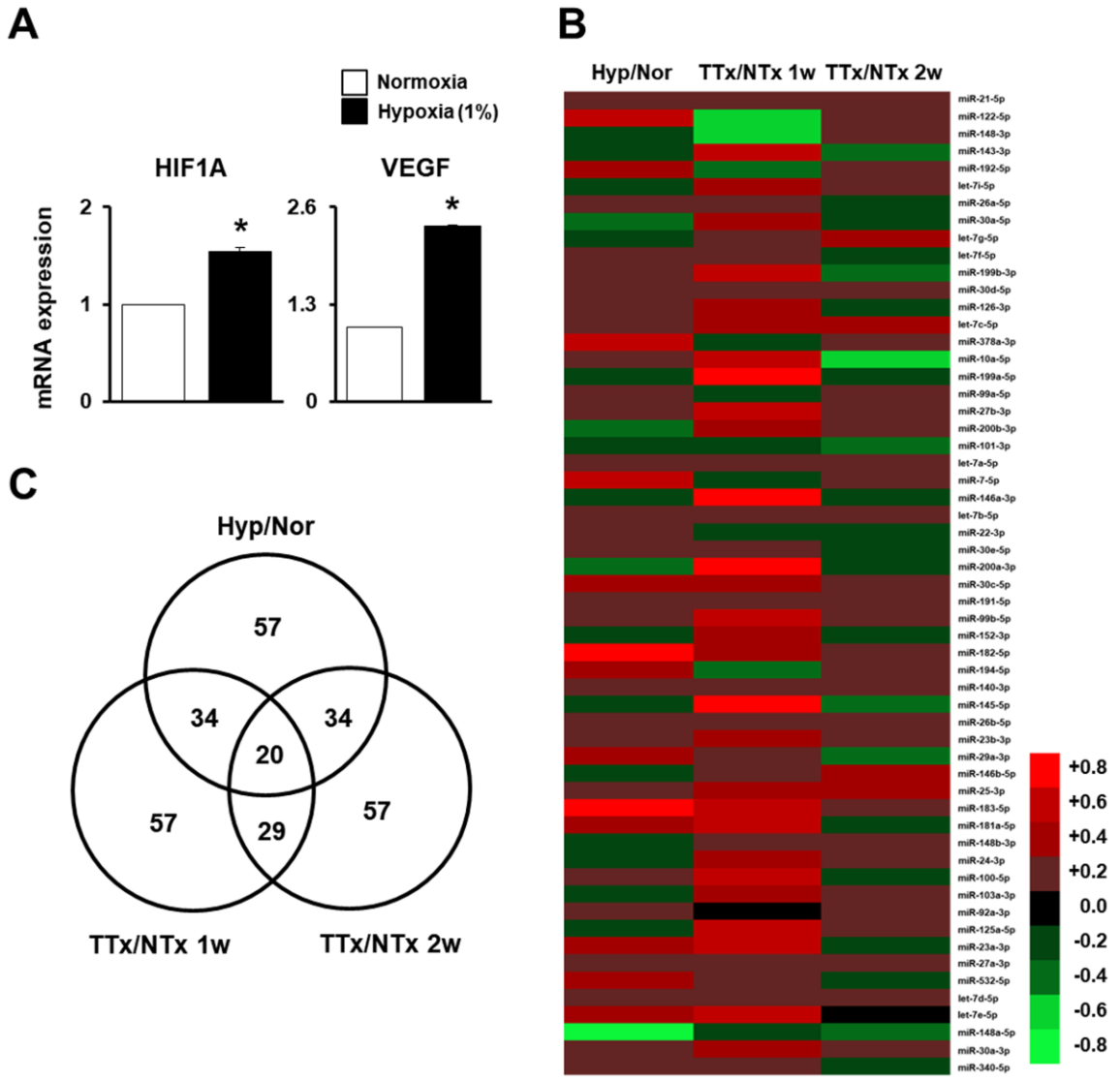


**Figure 1.** miRNA profiling of invaded naïve placenta-derived mesenchymal stem cells (PD-MSCs) under hypoxic conditions and in bile duct ligation (BDL)-injured liver in rats. (A) mRNA expression of hypoxia-inducible factor 1 alpha (HIF1A) and vascular endothelial growth factor (VEGF) in invaded naïve PD-MSCs determined using a Transwell insert system under 1% hypoxic conditions for 24 h and by quantitative real-time polymerase chain reaction (qRT-PCR). (B) Heat map and (C) Venn diagram of the microarray results of naïve PD-MSCs under hypoxic conditions compared with normoxic conditions (Hyp/Nor), TTx Naïve compared to NTx at 1 week (TTx/NTx 1w), and TTx Naïve compared to NTx at 2 weeks (TTx/NTx 2w). Data from each group are shown as the mean ± SD. * $p < 0.05$ vs. normoxia.

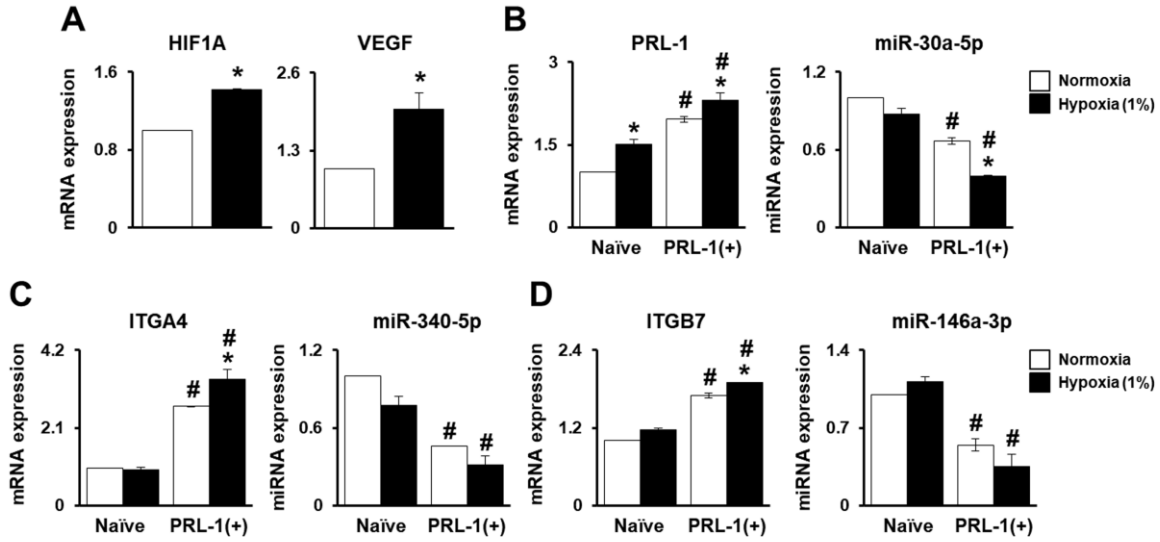


**Figure 2.** Phosphatase of regenerating liver-1 (PRL-1)-dependent migration ability under hypoxic conditions regulated by miRNAs targeting the integrin family. (A) mRNA expression of HIF1A and VEGF in invaded PRL-1(+) PD-MSCs determined using a Transwell insert system under 1% hypoxic conditions for 24 h and by qRT-PCR. (B) mRNA expression levels of PRL-1 and targeted hsa-miR-30a-5p expression, (C) Integrin alpha 4 (ITGA4) and targeted hsa-miR-340-5p expression, and (D) Integrin beta 7 (ITGB7) and targeted hsa-miR-146a-3p expression in invaded PRL-1(+) PD-MSCs under 1% hypoxic conditions for 24 h as determined by qRT-PCR. Data from each group are expressed as the mean ± SD. $^{*}$ $p < 0.05$ vs. normoxia and $^{\#}$ $p < 0.05$ vs. naïve.

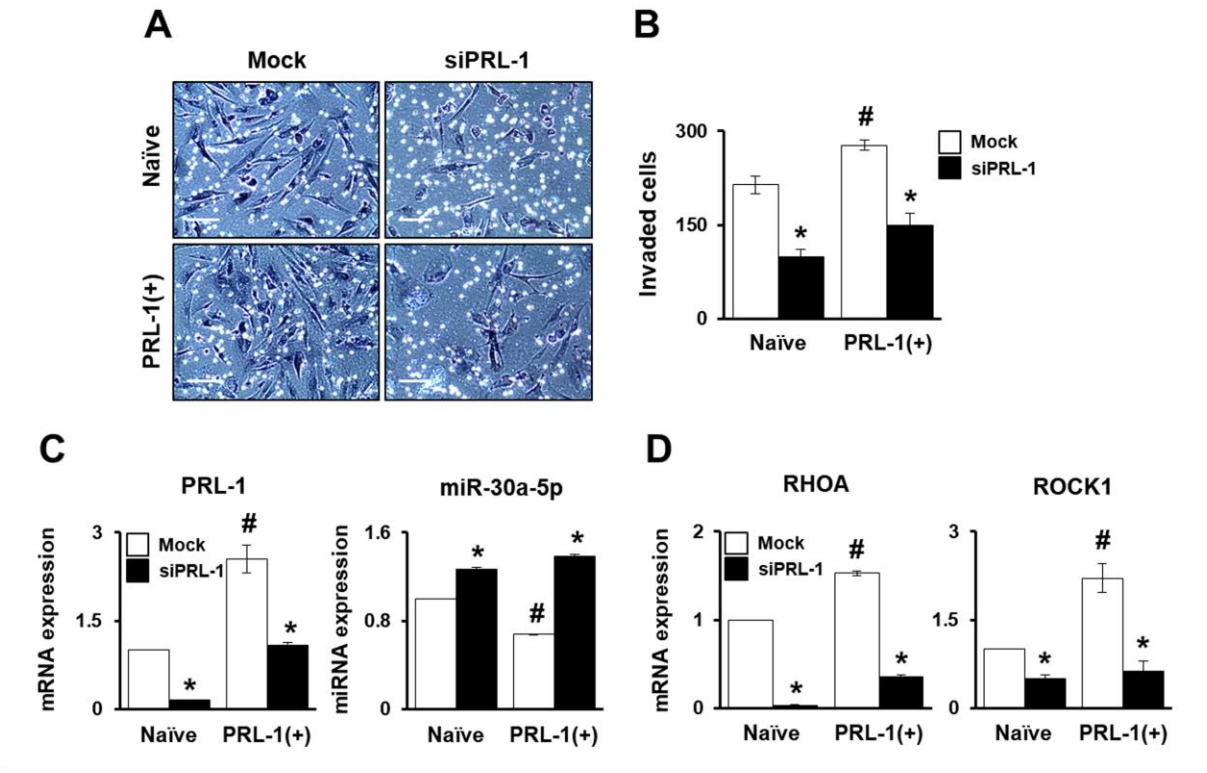


452

453 **Figure 3.** PRL-1-Targeted miRNA expression regulates migration ability through the RHO family.
454 (A) Representative images and (B) the number of invaded cells in invaded naïve PD-MSCs and PRL-
455 1(+) PD-MSCs determined using a Transwell insert system following siRNA-PRL-1 (siPRL-1)
456 treatment (50 nM) for 24 h. (C) mRNA expression of PRL-1 and targeted hsa-miR-30a-5p expression
457 and (D) Ras homolog family member A (RHOA) and Rho-associated coiled-coil-containing protein
458 kinase 1 (ROCK1) in invaded naïve and PRL-1(+) PD-MSCs determined using a Transwell insert
459 system following siPRL-1 treatment (50 nM) for 24 h as determined by qRT-PCR. Data from each
460 group are shown as the mean ± SD. Scale bars = 100 μm. * $p < 0.05$ vs. mock and # $p < 0.05$ vs. naïve.

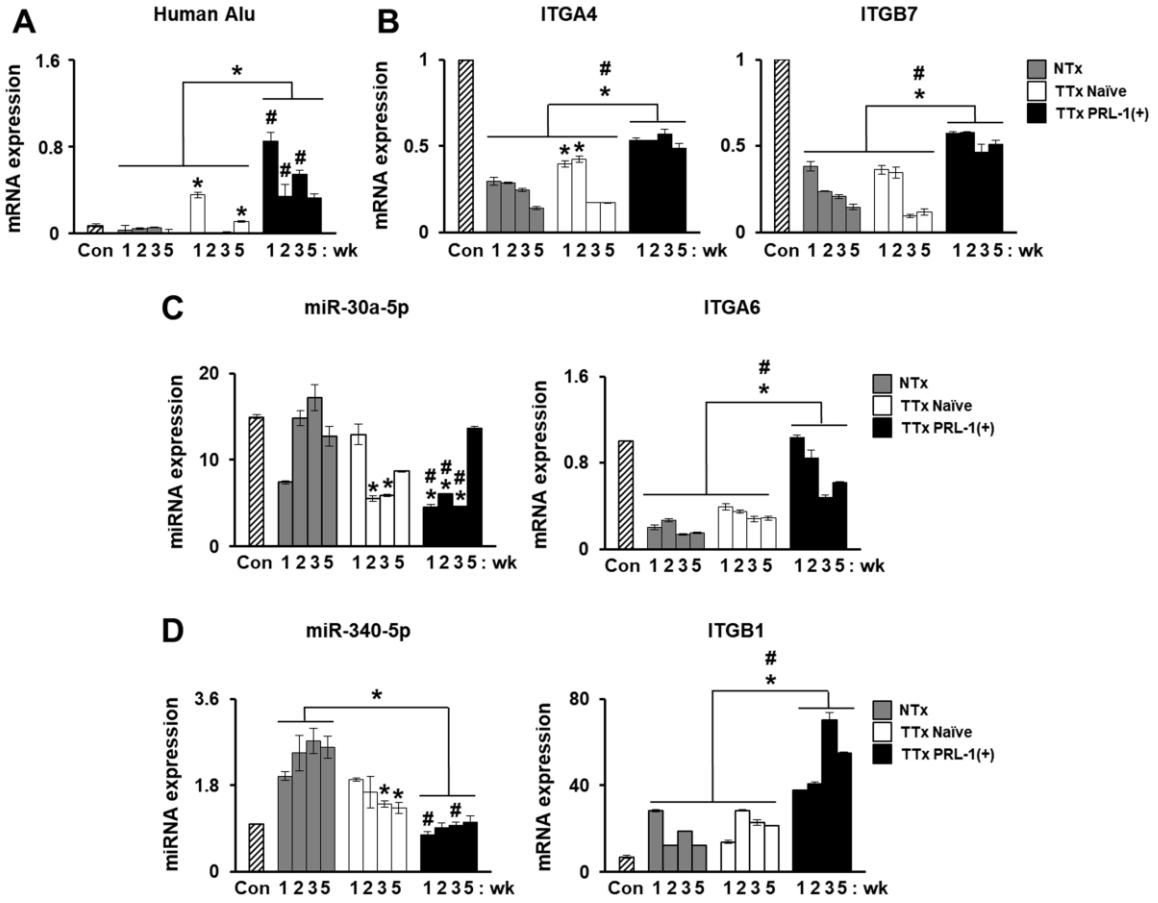


**Figure 4.** Integrin family regulates miRNA expression for PRL-1(+) PD-MSC homing in vivo in a rat model of BDL. mRNA expression levels of (A) human-specific Alu sequence, (B) ITGA4 and ITGB7 after the engraftment of naïve (TTx Naïve) and PRL-1(+) PD-MSCs (TTx PRL-1(+)) into injured rat liver compared with the sham control (Con) and BDL-injured nontransplantation groups (NTx) at 1, 2, 3, and 5 weeks as determined by qRT-PCR. (C) Integrin alpha 6 (ITGA6)-targeted rno-miR-30a-5p and (D) Integrin beta 1 (ITGB1)-targeted rno-miR-340-5p expression in rat liver with BDL at 1, 2, 3, and 5 weeks post-transplantation as determined by qRT-PCR. Data from each group are shown as the mean ± SD. $^{*}$ $p < 0.05$ vs. NTx and $^{\#}$ $p < 0.05$ vs. TTx Naïve.

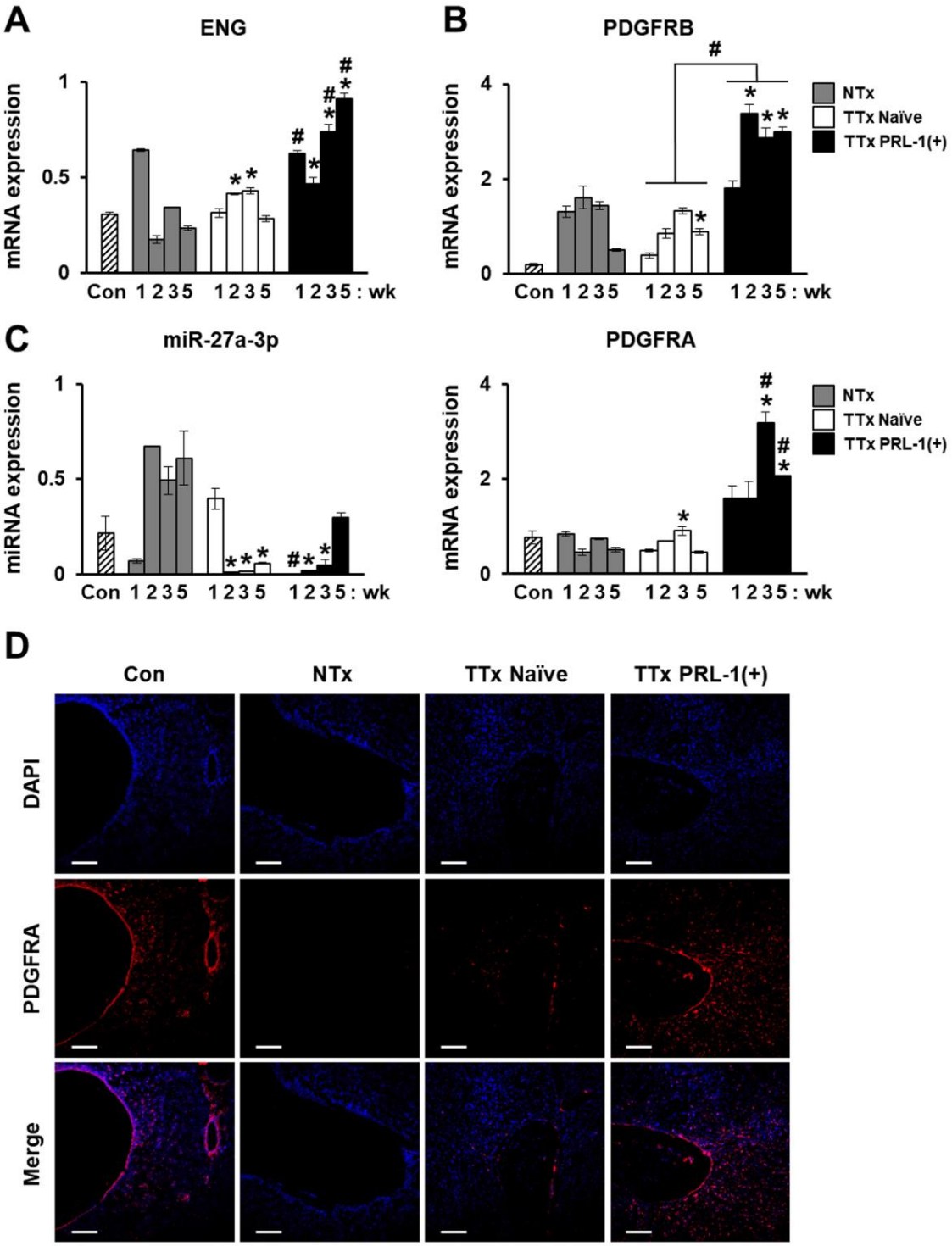


471

472 **Figure 5.** Improved vascular remodeling by PRL-1(+) PD-MSCs through the regulation of miRNA
473 expression by platelet-derived growth factor receptor alpha (PDGFRA) in a BDL-injured rat model.
474 (A) qRT-PCR of endoglin (ENG) and (B) platelet-derived growth factor receptor beta (PDGFRB)

and (C) PDGFRA-targeted rno-miR-27a-3p expression in BDL-injured rat liver tissue after the administration of naïve and PRL-1(+) PD-MSCs at 1, 2, 3, and 5 weeks. (D) Localization of PDGFRA expression in rat liver sections from each group (Con, NTx, TTx Naïve, and TTx PRL-1(+)) at 1 week as determined by immunofluorescence (red, PDGFRA; blue, DAPI). Scale bars = 100 μm. Data from each group are expressed as the mean ± SD. $^{*}$ $p < 0.05$ vs. NTx and $^{\#}$ $p < 0.05$ vs. TTx Naïve.

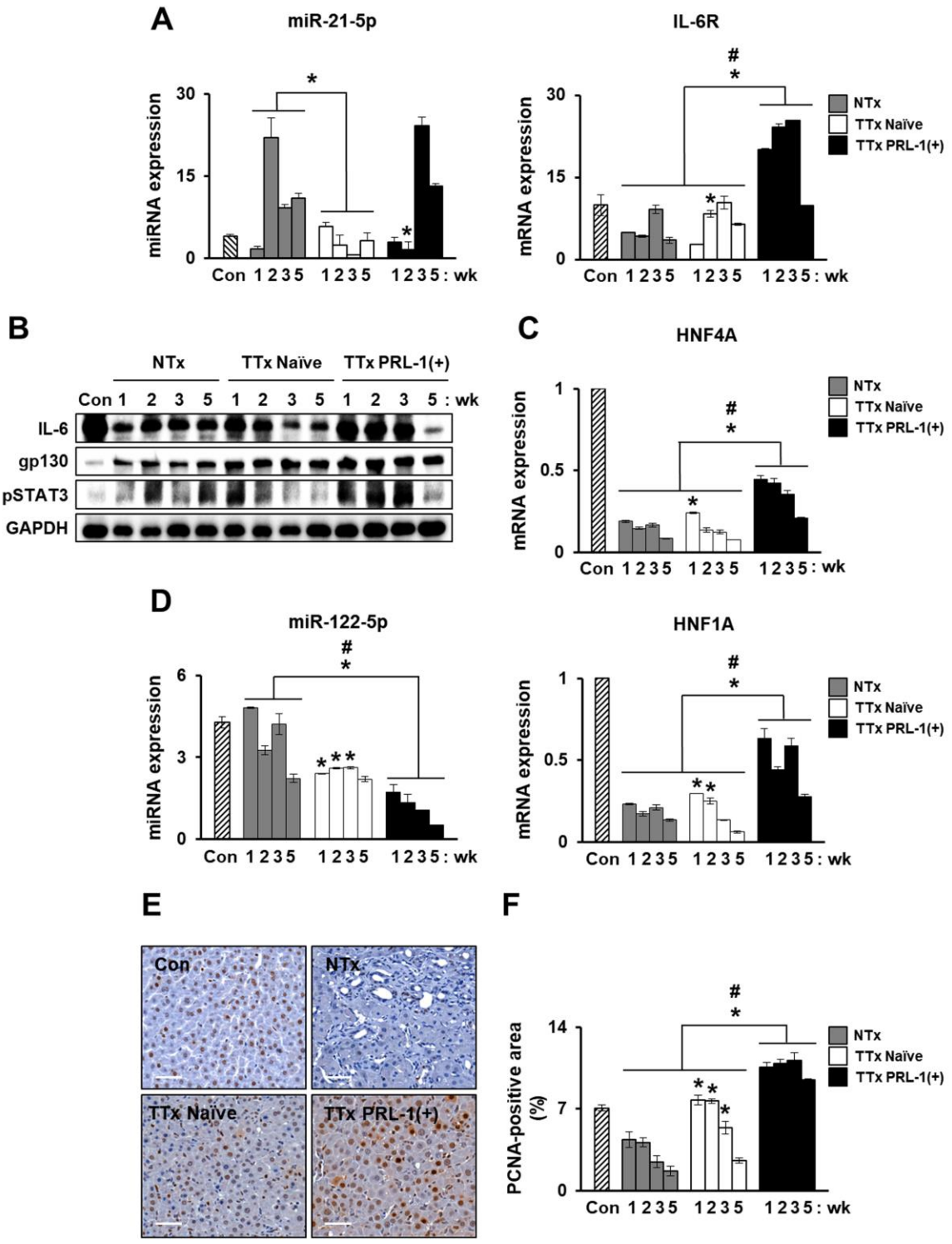


**Figure 6.** miRNAs mediated hepatic regeneration by PRL-1(+) PD-MSCs in a rat model of BDL through interleukin-6 (IL-6)/signal transducer and activator of transcription 3 (STAT3) signaling. (A) qRT-PCR of rno-miR-21-5p-targeted interleukin-6 receptor (IL-6R) and (B) western blotting of glycoprotein 130 (gp130), IL-6, and phosphorylated STAT3 levels in BDL-injured rat liver tissue

following the administration of naïve and PRL-1(+) PD-MSCs at 1, 2, 3, and 5 weeks. (C) mRNA expression of hepatocyte nuclear factor 4 alpha (HNF4A) and (D) miR-122-5p-targeted HNF1 homeobox A (HNF1A) in BDL-injured rat liver tissue by qRT-PCR. (E) Proliferating cell nuclear antigen (PCNA) expression in the rat liver sections from each group (Con, NTx, TTx Naïve, and TTx PRL-1(+)) at 1 week as determined by immunohistochemistry. (F) Quantification of the PCNA-positive area in hepatocytes. Scale bars = 50 μm. Data from each group are expressed as the mean ± SD. $^{*}$ $p < 0.05$ vs. NTx, $^{\#}$ $p < 0.05$ vs. TTx Naïve.

**Table S1**: Primer sequences for human using quantitative real time polymerase chain reaction

| Gene | Accession Number | Sequence | Tm (℃) |
|---|---|---|---|
| HIF1A | NM_001530.4 | F: 5'-GTTTACTAAAGGACAAGTCA-3'<br>R: 5'-TTCTGTTTGTTGAAGGGAG-3' | 60 |
| VEGF | NM_001204384.1 | F: 5'-GCCTTGCCTTGCTGCTCTAC-3'<br>R: 5'-ACATCCATGAACTTCACCACTTCG-3' | 60 |
| PRL-1 | NM_003463.4 | F: 5'-TACTGCTCCACCAAGAAGCC-3'<br>R: 5'-AGGTTTACCCCATCCAGGTC-3' | 60 |
| ITGA4 | NM_000885.6 | F: 5'-TTCCTACGGGCTGTGTTC-3'<br>R: 5'-CTGAAGTTTGCCAGTTTGG-3' | 55 |
| ITGB7 | NM_000889.3 | F: 5'-AGCAGCAACAACTCAACTGG-3'<br>R: 5'-TTACAGACCCACCCTTCCTCT-3' | 55 |
| RHOA | NM_001664.4 | F: 5'-TGGAAAGCAGGTAGAGTTGG-3'<br>R: 5'-GACTTCTGGGGTCCACTTTT-3' | 55 |
| ROCK1 | NM_005406.3 | F: 5'-GAAGAAAGAGAAGCTCGAGA-3'<br>R: 5'-GATCTTGTAGCTCCCGCATCTGT-3' | 55 |
| GAPDH | NM_002046.7 | F: 5'-GCACCGTCAAGGCTGAGAAC-3'<br>R: 5'-GTGGTGAAGACGCCAGTGGA-3' | 60 |

499 **Table S2:** Primer sequences for rat using quantitative real time polymerase chain reaction

| Gene | Accession Number | Sequence | Tm (℃) |
|---|---|---|---|
| ITGA4 | NM_001107737.1 | F: 5'-GGAAGCCCCAGTGGAGAAC-3'<br>R: 5'-ATTGTCACTCCCAGCCACTGA-3' | 55 |
| ITGA6 | NM_053725.1 | F: 5'-AGCCCCAGGGACTTACAACT-3'<br>R: 5'-CTTCATAGGGCCCATCTTCA-3' | 55 |
| ITGB1 | NM_017022.2 | F: 5'-AACAGTGAAGACATGGATGC-3'<br>R: 5'-CTCTCTCTTCCTGCACACAC-3' | 55 |
| ITGB7 | NM_013171.1 | F: 5'-AGTGCCCTCCAAGCTTAACCAC-3'<br>R: 5'-CGTCCCACCTCTCTCTCGAA-3' | 55 |
| ENG | NM_001010968.2 | F: 5'-AAGGTGTGACTGGACACAAG-3'<br>R: 5'-CCAGATCTGCATATTGTGGT-3' | 60 |
| PDGFRA | NM_012802.1 | F: 5'-GAGGACGATTCTGCCATCAT-3'<br>R: 5'-CAGTTCTGACGTGGCTTTCA-3' | 60 |
| PDGFRB | NM_031525.1 | F: 5'-TGTTCGTGCTATTGCTCCTG-3'<br>R: 5'-TGTCAGCACACTGGAGAAGG-3' | 60 |
| IL-6R | NM_017020.3 | F: 5'-CCTTGTAAATGCCTTTTGTG-3'<br>R: 5'-GTACACTTTGTCACCCTCCA-3' | 60 |
| HNF1A | NM_012669.1 | F: 5'-AAGATGACACGGATGACGATGG-3'<br>R: 5'-GGTTGAGACCCGTAGTGTCC-3' | 60 |
| HNF4A | NM_022180.2 | F: 5'-AAATGTGCAGGTGTTGACCA-3'<br>R: 5'-CACGCTCCTCCTGAAGAATC-3' | 60 |
| GAPDH | NM_017008.4 | F: 5'-TCCCTCAAGATTGTCAGCAA-3'<br>R: 5'-AGATCCACAACGGATACATT-3' | 60 |

500

501

502 **Table S3**: miRNA sequence and target gene in 3' UTR site

| miRNA Target Gene | Accession Number | Target Sequence |
|---|---|---|
| hsa-miR-30a-5p | MIMAT0000087 | 3'-GAAGGUCAGCUCCU**ACAAAUGU**-5' |
| hPRL-1 | NM_003463.4 | 5'-GCCUGCUCACUUUA**UGUUUACA**-3' |
| hITGA4 | NM_000885.6 | 5'-AAUUUAAAAGACAC**UGUUUACA**-3' |
| hsa-miR-340-5p | MIMAT0004692 | 3'-UUAGUCAGAGUAACG**AAAUAUU**-5' |
| hITGA4 | NM_000885.6 | 5'-CUUUAAAGCCCUUUA**UUUAUAA**-3' |
| hsa-miR-146a-3p | MIMAT0004608 | 3'-GACUUCUUGACUUA**AAGUCUC**C-5' |
| hITGB7 | NM_000889.3 | 5'-CACCCUACUUCAUU**UUCAGAG**U-3' |
| rno-miR-340-5p | MIMAT0004650 | 3'-UUAGUCAGAGUAAC**GAAAUAUU**-5' |
| rITGB1 | NM_017022.2 | 5'-UCCCAACGCCUUCU**CUUUAUAA**-3' |
| rno-miR-30a-5p | MIMAT0000808 | 3'-GAAGGUCAGCUCCU**ACAAAUGU**-5' |
| rITGA6 | NM_053725.1 | 5'-UACAAAUGAUGCCU**UGUUUACA**-3' |
| rno-miR-27a-3p | MIMAT0000799 | 3'-CGCCUUGAAUCGGU**GACACUU**-5' |
| rPDGFRA | NM_012802.1 | 5'-GUCUUGGGAAGCCU**CUGUGAA**-3' |
| rno-miR-21-5p | MIMAT0000790 | 3'-AGUUGUAGUCAGAC**UAUUCGAU**-5' |
| rIL-6R | NM_017020.3 | 5'-CCUUUUGACUUUUU**AUAAGCUA**-3' |
| rno-miR-122-5p | MIMAT0000827 | 3'-GUUUGUGGUAACAGU**GUGAGG**U-5' |
| rHNF1A | NM_001530.4 | 5'-CCUGUGCCUCCCAGG**CCACUCC**A-3' |

503

## References


1. Friedman, S.L. Mechanisms of hepatic fibrogenesis. *Gastroenterology* **2008**, *134*, 1655-1669, doi:10.1053/j.gastro.2008.03.003.
2. Praktiknjo, M.; Lehmann, J.; Nielsen, M.J.; Schierwagen, R.; Uschner, F.E.; Meyer, C.; Thomas, D.; Strassburg, C.P.; Bendtsen, F.; Moller, S., et al. Acute decompensation boosts hepatic collagen type III deposition and deteriorates experimental and human cirrhosis. *Hepatol Commun* **2018**, *2*, 211-222, doi:10.1002/hep4.1135.
3. Friedman, S.L.; Sheppard, D.; Duffield, J.S.; Violette, S. Therapy for fibrotic diseases: nearing the starting line. *Sci Transl Med* **2013**, *5*, 167sr161, doi:10.1126/scitranslmed.3004700.
4. Liu, L.; Yannam, G.R.; Nishikawa, T.; Yamamoto, T.; Basma, H.; Ito, R.; Nagaya, M.; Dutta-Moscato, J.; Stolz, D.B.; Duan, F., et al. The microenvironment in hepatocyte regeneration and function in rats with advanced cirrhosis. *Hepatology* **2012**, *55*, 1529-1539, doi:10.1002/hep.24815.
5. Arany, Z.; Foo, S.Y.; Ma, Y.; Ruas, J.L.; Bommi-Reddy, A.; Girnun, G.; Cooper, M.; Laznik, D.; Chinsomboon, J.; Rangwala, S.M., et al. HIF-independent regulation of VEGF and angiogenesis by the transcriptional coactivator PGC-1alpha. *Nature* **2008**, *451*, 1008-1012, doi:10.1038/nature06613.
6. Lee, D.S.; Gil, W.H.; Lee, H.H.; Lee, K.W.; Lee, S.K.; Kim, S.J.; Choi, S.H.; Heo, J.S.; Hyon, W.S.; Kim, G.S., et al. Factors affecting graft survival after living donor liver transplantation. *Transplant Proc* **2004**, *36*, 2255-2256, doi:10.1016/j.transproceed.2004.08.073.
7. Yukawa, H.; Noguchi, H.; Oishi, K.; Takagi, S.; Hamaguchi, M.; Hamajima, N.; Hayashi, S. Cell transplantation of adipose tissue-derived stem cells in combination with heparin attenuated acute liver failure in mice. *Cell Transplant* **2009**, *18*, 611-618.
8. Abdel aziz, M.T.; El Asmar, M.F.; Atta, H.M.; Mahfouz, S.; Fouad, H.H.; Roshdy, N.K.; Rashed, L.A.; Sabry, D.; Hassouna, A.A.; Taha, F.M. Efficacy of mesenchymal stem cells in suppression of hepatocarcinorigenesis in rats: possible role of Wnt signaling. *J Exp Clin Cancer Res* **2011**, *30*, 49, doi:10.1186/1756-9966-30-49.
9. Jung, J.; Choi, J.H.; Lee, Y.; Park, J.W.; Oh, I.H.; Hwang, S.G.; Kim, K.S.; Kim, G.J. Human placenta-derived mesenchymal stem cells promote hepatic regeneration in CCl4 -injured rat liver model via increased autophagic mechanism. *Stem Cells* **2013**, *31*, 1584-1596, doi:10.1002/stem.1396.
10. Jung, J.; Moon, J.W.; Choi, J.H.; Lee, Y.W.; Park, S.H.; Kim, G.J. Epigenetic Alterations of IL-6/STAT3 Signaling by Placental Stem Cells Promote Hepatic Regeneration in a Rat Model with CCl4-induced Liver Injury. *Int J Stem Cells* **2015**, *8*, 79-89, doi:10.15283/ijsc.2015.8.1.79.
11. Haider, H.; Jiang, S.; Idris, N.M.; Ashraf, M. IGF-1-overexpressing mesenchymal stem cells accelerate bone marrow stem cell mobilization via paracrine activation of SDF-1alpha/CXCR4 signaling to promote myocardial repair. *Circ Res* **2008**, *103*, 1300-1308, doi:10.1161/CIRCRESAHA.108.186742.
12. Teo, G.S.; Ankrum, J.A.; Martinelli, R.; Boetto, S.E.; Simms, K.; Sciuto, T.E.; Dvorak, A.M.; Karp, J.M.; Carman, C.V. Mesenchymal stem cells transmigrate between and directly through tumor necrosis factor-alpha-activated endothelial cells via both leukocyte-like and novel mechanisms. *Stem Cells* **2012**, *30*, 2472-2486, doi:10.1002/stem.1198.
13. Choi, J.H.; Lim, S.M.; Yoo, Y.I.; Jung, J.; Park, J.W.; Kim, G.J. Microenvironmental Interaction Between Hypoxia and Endothelial Cells Controls the Migration Ability of

Placenta-Derived Mesenchymal Stem Cells via alpha4 Integrin and Rho Signaling. *J Cell Biochem* **2016**, *117*, 1145-1157, doi:10.1002/jcb.25398.

14. Wang, D.; Li, L.K.; Dai, T.; Wang, A.; Li, S. Adult Stem Cells in Vascular Remodeling. *Theranostics* **2018**, *8*, 815-829, doi:10.7150/thno.19577.
15. Mueller, L.; Broering, D.C.; Meyer, J.; Vashist, Y.; Goettsche, J.; Wilms, C.; Rogiers, X. The induction of the immediate-early-genes Egr-1, PAI-1 and PRL-1 during liver regeneration in surgical models is related to increased portal flow. *J Hepatol* **2002**, *37*, 606-612.
16. Peng, Y.; Du, K.; Ramirez, S.; Diamond, R.H.; Taub, R. Mitogenic up-regulation of the PRL-1 protein-tyrosine phosphatase gene by Egr-1. Egr-1 activation is an early event in liver regeneration. *J Biol Chem* **1999**, *274*, 4513-4520, doi:10.1074/jbc.274.8.4513.
17. Achiwa, H.; Lazo, J.S. PRL-1 tyrosine phosphatase regulates c-Src levels, adherence, and invasion in human lung cancer cells. *Cancer Res* **2007**, *67*, 643-650, doi:10.1158/0008-5472.CAN-06-2436.
18. Bai, Y.; Luo, Y.; Liu, S.; Zhang, L.; Shen, K.; Dong, Y.; Walls, C.D.; Quilliam, L.A.; Wells, C.D.; Cao, Y., et al. PRL-1 protein promotes ERK1/2 and RhoA protein activation through a non-canonical interaction with the Src homology 3 domain of p115 Rho GTPase-activating protein. *J Biol Chem* **2011**, *286*, 42316-42324, doi:10.1074/jbc.M111.286302.
19. Dong, J.; Sui, L.; Wang, Q.; Chen, M.; Sun, H. MicroRNA-26a inhibits cell proliferation and invasion of cervical cancer cells by targeting protein tyrosine phosphatase type IVA 1. *Mol Med Rep* **2014**, *10*, 1426-1432, doi:10.3892/mmr.2014.2335.
20. Flores-Perez, A.; Marchat, L.A.; Rodriguez-Cuevas, S.; Bautista, V.P.; Fuentes-Mera, L.; Romero-Zamora, D.; Maciel-Dominguez, A.; de la Cruz, O.H.; Fonseca-Sanchez, M.; Ruiz-Garcia, E., et al. Suppression of cell migration is promoted by miR-944 through targeting of SIAH1 and PTP4A1 in breast cancer cells. *BMC Cancer* **2016**, *16*, 379, doi:10.1186/s12885-016-2470-3.
21. Hu, J.Y.; Yi, W.; Wei, X.; Zhang, M.Y.; Xu, R.; Zeng, L.S.; Huang, Z.J.; Chen, J.S. miR-601 is a prognostic marker and suppresses cell growth and invasion by targeting PTP4A1 in breast cancer. *Biomed Pharmacother* **2016**, *79*, 247-253, doi:10.1016/j.biopha.2016.02.014.
22. Li, Z.; Rana, T.M. Therapeutic targeting of microRNAs: current status and future challenges. *Nat Rev Drug Discov* **2014**, *13*, 622-638, doi:10.1038/nrd4359.
23. Li, N.; Long, B.; Han, W.; Yuan, S.; Wang, K. microRNAs: important regulators of stem cells. *Stem Cell Res Ther* **2017**, *8*, 110, doi:10.1186/s13287-017-0551-0.
24. Chang, N.; Ge, J.; Xiu, L.; Zhao, Z.; Duan, X.; Tian, L.; Xie, J.; Yang, L.; Li, L. HuR mediates motility of human bone marrow-derived mesenchymal stem cells triggered by sphingosine 1-phosphate in liver fibrosis. *J Mol Med (Berl)* **2017**, *95*, 69-82, doi:10.1007/s00109-016-1460-x.
25. Bi, Z.M.; Zhou, Q.F.; Geng, Y.; Zhang, H.M. Human umbilical cord mesenchymal stem cells ameliorate experimental cirrhosis through activation of keratinocyte growth factor by suppressing microRNA-199. *Eur Rev Med Pharmacol Sci* **2016**, *20*, 4905-4912.
26. Nitzsche, F.; Muller, C.; Lukomska, B.; Jolkkonen, J.; Deten, A.; Boltze, J. Concise Review: MSC Adhesion Cascade-Insights into Homing and Transendothelial Migration. *Stem Cells* **2017**, *35*, 1446-1460, doi:10.1002/stem.2614.
27. Xu, B.; Song, G.; Ju, Y.; Li, X.; Song, Y.; Watanabe, S. RhoA/ROCK, cytoskeletal dynamics, and focal adhesion kinase are required for mechanical stretch-induced

tenogenic differentiation of human mesenchymal stem cells. *J Cell Physiol* **2012**, *227*, 2722-2729, doi:10.1002/jcp.23016.

28. Eom, Y.W.; Shim, K.Y.; Baik, S.K. Mesenchymal stem cell therapy for liver fibrosis. *Korean J Intern Med* **2015**, *30*, 580-589, doi:10.3904/kjim.2015.30.5.580.
29. Alfaifi, M.; Eom, Y.W.; Newsome, P.N.; Baik, S.K. Mesenchymal stromal cell therapy for liver diseases. *J Hepatol* **2018**, *68*, 1272-1285, doi:10.1016/j.jhep.2018.01.030.
30. Clark, E.A.; Kalomoiris, S.; Nolta, J.A.; Fierro, F.A. Concise review: MicroRNA function in multipotent mesenchymal stromal cells. *Stem Cells* **2014**, *32*, 1074-1082.
31. Saller, M.M.; Prall, W.C.; Docheva, D.; Schonitzer, V.; Popov, T.; Anz, D.; Clausen-Schaumann, H.; Mutschler, W.; Volkmer, E.; Schieker, M., et al. Increased stemness and migration of human mesenchymal stem cells in hypoxia is associated with altered integrin expression. *Biochem Biophys Res Commun* **2012**, *423*, 379-385, doi:10.1016/j.bbrc.2012.05.134.
32. Choi, J.H.; Lee, Y.B.; Jung, J.; Hwang, S.G.; Oh, I.H.; Kim, G.J. Hypoxia Inducible Factor-1alpha Regulates the Migration of Bone Marrow Mesenchymal Stem Cells via Integrin alpha 4. *Stem Cells Int* **2016**, *2016*, 7932185, doi:10.1155/2016/7932185.
33. Luo, Y.; Liang, F.; Zhang, Z.Y. PRL1 promotes cell migration and invasion by increasing MMP2 and MMP9 expression through Src and ERK1/2 pathways. *Biochemistry* **2009**, *48*, 1838-1846, doi:10.1021/bi8020789.
34. Wang, Y.; Lazo, J.S. Metastasis-associated phosphatase PRL-2 regulates tumor cell migration and invasion. *Oncogene* **2012**, *31*, 818-827, doi:10.1038/onc.2011.281.
35. Gari, H.H.; DeGala, G.D.; Ray, R.; Lucia, M.S.; Lambert, J.R. PRL-3 engages the focal adhesion pathway in triple-negative breast cancer cells to alter actin structure and substrate adhesion properties critical for cell migration and invasion. *Cancer Lett* **2016**, *380*, 505-512, doi:10.1016/j.canlet.2016.07.017.
36. Guan, J.L. Integrin signaling through FAK in the regulation of mammary stem cells and breast cancer. *IUBMB Life* **2010**, *62*, 268-276, doi:10.1002/iub.303.
37. Vitillo, L.; Kimber, S.J. Integrin and FAK Regulation of Human Pluripotent Stem Cells. *Curr Stem Cell Rep* **2017**, *3*, 358-365, doi:10.1007/s40778-017-0100-x.
38. Drescher, H.K.; Schippers, A.; Clahsen, T.; Sahin, H.; Noels, H.; Hornef, M.; Wagner, N.; Trautwein, C.; Streetz, K.L.; Kroy, D.C. beta7-Integrin and MAdCAM-1 play opposing roles during the development of non-alcoholic steatohepatitis. *J Hepatol* **2017**, *66*, 1251-1264, doi:10.1016/j.jhep.2017.02.001.
39. Aldridge, V.; Garg, A.; Davies, N.; Bartlett, D.C.; Youster, J.; Beard, H.; Kavanagh, D.P.; Kalia, N.; Frampton, J.; Lalor, P.F., et al. Human mesenchymal stem cells are recruited to injured liver in a beta1-integrin and CD44 dependent manner. *Hepatology* **2012**, *56*, 1063-1073, doi:10.1002/hep.25716.
40. Chute, J.P. Stem cell homing. *Curr Opin Hematol* **2006**, *13*, 399-406, doi:10.1097/01.moh.0000245698.62511.3d.
41. Amiri, F.; Molaei, S.; Bahadori, M.; Nasiri, F.; Deyhim, M.R.; Jalili, M.A.; Nourani, M.R.; Habibi Roudkenar, M. Autophagy-Modulated Human Bone Marrow-Derived Mesenchymal Stem Cells Accelerate Liver Restoration in Mouse Models of Acute Liver Failure. *Iran Biomed J* **2016**, *20*, 135-144.
42. Yang, L.; Dong, C.; Yang, J.; Yang, L.; Chang, N.; Qi, C.; Li, L. MicroRNA-26b-5p Inhibits Mouse Liver Fibrogenesis and Angiogenesis by Targeting PDGF Receptor-Beta. *Mol Ther Nucleic Acids* **2019**, *16*, 206-217, doi:10.1016/j.omtn.2019.02.014.
43. Jiao, Y.; Ye, D.Z.; Li, Z.; Teta-Bissett, M.; Peng, Y.; Taub, R.; Greenbaum, L.E.; Kaestner, K.H. Protein tyrosine phosphatase of liver regeneration-1 is required for

652 normal timing of cell cycle progression during liver regeneration. *Am J Physiol*
653 *Gastrointest Liver Physiol* **2015**, *308*, G85-91, doi:10.1152/ajpgi.00084.2014.
654 44. Ding, W.; Xin, J.; Jiang, L.; Zhou, Q.; Wu, T.; Shi, D.; Lin, B.; Li, L.; Li, J.
655 Characterisation of peripheral blood mononuclear cell microRNA in hepatitis B-
656 related acute-on-chronic liver failure. *Sci Rep* **2015**, *5*, 13098, doi:10.1038/srep13098.
657 45. Hu, J.; Xu, Y.; Hao, J.; Wang, S.; Li, C.; Meng, S. MiR-122 in hepatic function and
658 liver diseases. *Protein Cell* **2012**, *3*, 364-371, doi:10.1007/s13238-012-2036-3.
659 46. Lou, G.; Yang, Y.; Liu, F.; Ye, B.; Chen, Z.; Zheng, M.; Liu, Y. MiR-122
660 modification enhances the therapeutic efficacy of adipose tissue-derived
661 mesenchymal stem cells against liver fibrosis. *J Cell Mol Med* **2017**, *21*, 2963-2973,
662 doi:10.1111/jcmm.13208.
663 47. Baranova, A.; Maltseva, D.; Tonevitsky, A. Adipose may actively delay progression
664 of NAFLD by releasing tumor-suppressing, anti-fibrotic miR-122 into circulation.
665 *Obes Rev* **2019**, *20*, 108-118, doi:10.1111/obr.12765.
666 48. Kim, M.J.; Shin, K.S.; Jeon, J.H.; Lee, D.R.; Shim, S.H.; Kim, J.K.; Cha, D.H.; Yoon,
667 T.K.; Kim, G.J. Human chorionic-plate-derived mesenchymal stem cells and
668 Wharton's jelly-derived mesenchymal stem cells: a comparative analysis of their
669 potential as placenta-derived stem cells. *Cell Tissue Res* **2011**, *346*, 53-64,
670 doi:10.1007/s00441-011-1249-8.
671 49. Lee, H.J.; Jung, J.; Cho, K.J.; Lee, C.K.; Hwang, S.G.; Kim, G.J. Comparison of in
672 vitro hepatogenic differentiation potential between various placenta-derived stem
673 cells and other adult stem cells as an alternative source of functional hepatocytes.
674 *Differentiation* **2012**, *84*, 223-231, doi:10.1016/j.diff.2012.05.007.
675 50. Kountouras, J.; Billing, B.H.; Scheuer, P.J. Prolonged bile duct obstruction: a new
676 experimental model for cirrhosis in the rat. *Br J Exp Pathol* **1984**, *65*, 305-311.

677